

Perfect Nonradiating Modes in Dielectric Nanoparticles

Vasily V. Klimov

P.N. Lebedev Physical Institute, Russian Academy of Sciences, 53 Leninsky Prospekt,

Moscow 119991, Russia

E-mail: klimov256@gmail.com

Abstract

A general concept of perfect nonradiating modes in dielectric nanoparticles of an arbitrary shape is put forward. It is proved that such modes exist in axisymmetric dielectric nanoparticles and have unlimited radiative Q -factors. With smart tuning of the excitation beams, perfect modes appear as deep minima in the scattered radiation spectra (up to complete disappearance), but at the same time they have a giant amplification of the fields inside the particle. Such modes have no analogues and can be useful for the realization of low threshold nanolasers and other strong nonlinear effects in nanoparticles.

At present, the properties of dielectric nanoparticles with a high refractive index and low radiative losses are being actively investigated [1-9]. The physics of optical phenomena in such nanoparticles is very complicated and leads to many interesting applications, such as nano-antennas [1-3], nanolasers [4,5] and nonlinear nanophotonics [8,9]. As in any other field of physics, all these phenomena are associated with the existence of certain eigenmodes in nanoparticles.

For applications, modes with strong field localization and low radiation losses are of particular interest. This kind of modes had attracted the closest attention of the leading scientific groups, discovered several types of weakly radiating phenomena: BIC modes [10-15], anapole states [8,10,16-23], supercavity modes [5, 24, 25], pseudo-modes [26], embedded photonic eigenvalues [27]. In this letter, we show that there are unparalleled perfect nonradiating modes in dielectric nanoparticles and we propose a regular method for finding such modes in arbitrary dielectric particles.

Usually, the eigenmodes are found by solving sourceless Maxwell's equations with the Sommerfeld radiation conditions at infinity [28], and therefore such modes are fundamentally

related to radiation losses. Moreover, such modes grow unlimitedly at infinity, requiring the development of very complex artificial approaches for their use, see e.g. [29-36] .

However, finding all the modes is a non-trivial task, not only from a computational point of view, and the modes investigated in the abovementioned works do not exhaust the entire set of modes that exist in dielectric particles. In this paper, we present a new class of eigenmodes - perfect nonradiating modes, and, to find them, we propose to use the solutions of Maxwell's equations, not containing waves that carry energy away in principle!

More specifically, we suggest to look for the electromagnetic field outside the particle in the form of a superposition of solutions of the Maxwell equations that are nonsingular in unlimited free space, including the interior of the nanoparticle. This approach is fundamentally different from the usual one, assuming that the functions describing the fields outside the body can have singularities upon analytic continuation into its interior. For example, expanding any field component $E(r, \theta, \varphi, \omega)$ outside the resonator over spherical harmonics $Y_n^m(\theta, \varphi)$ in accordance with the Sommerfeld radiation condition, usually one uses spherical Hankel functions $h_n^{(1)}(k_0 r)$ singular at $r = 0$ (inside the resonator):

$$E(r, \theta, \varphi, \omega) \sim \sum a_{nm} h_n^{(1)}(k_0 r) Y_n^m(\theta, \varphi) \quad (1),$$

fundamentally related to radiation. We propose, however, to find perfect nonradiating modes to use only the components nonsingular at the origin to describe the fields at infinity

$$E(r, \theta, \varphi, \omega) \sim \sum a_{nm} j_n(k_0 r) Y_n^m(\theta, \varphi) \quad (2)$$

where $j_n(k_0 r)$ are nonsingular spherical Bessel functions. Obviously, if such a solution exists, then, in principle, it will not have a flux of energy and radiation at infinity!

Since (2) has no singularities in the entire space (including the nanoparticle interior), finding of modes in infinite space can be reduced to finding fields in the volume of a nanoparticle only. As a result, the system of equations that determine the perfect nonradiating modes in a nanoparticle with the permittivity ε can be written as a system of two equations for two fields $\mathbf{E}_1, \mathbf{E}_2$ inside the particle:

$$\begin{aligned} \nabla \times \mathbf{E}_1 &= ik_0 \mathbf{H}_1; \nabla \times \mathbf{H}_1 = -ik_0 \varepsilon \mathbf{E}_1 \\ \nabla \times \mathbf{E}_2 &= ik_0 \mathbf{H}_2; \nabla \times \mathbf{H}_2 = -ik_0 \mathbf{E}_2 \end{aligned} \quad (3)$$

connected through the boundary conditions of continuity of the tangential components of the electric and magnetic fields

$$\mathbf{E}_{t,1} = \mathbf{E}_{t,2}; \mathbf{H}_{t,1} = \mathbf{H}_{t,2} \quad (4)$$

At some real values of frequency $\omega_n = k_{0,n} / c$ or permittivity ε_n , the system of equations (3),(4) becomes compatible, that is, perfect nonradiating modes appear. The fields inside the nanoparticle are determined by $\mathbf{E}_1, \mathbf{H}_1$, while the fields outside the particle are determined by the analytic continuation of the solution $\mathbf{E}_2, \mathbf{H}_2$.

Eigenmodes and eigenfrequencies found in this way have no analogues. In particular, they differ from the so-called anapole states [17-22,37] in that their fields outside the particle are different from zero and have a well-defined expansion in spherical harmonics (2). These modes also differ from the "bound states in a continuum" modes since they do not decay exponentially. Perfect modes are closest to strange Neumann-Wigner modes [38], but unlike the latter, the nanoparticle potential (permittivity) differs from vacuum value only in a finite region of space, distinguishing perfect nonradiating modes from Neumann-Wigner ones fundamentally [38].

The system of equations (3),(4) is very complicated, and a rigorous mathematical theory in a general case does not yet exist for it. Nevertheless, we managed to find conditions for the existence of perfect nonradiating modes for arbitrary spheroids and hyper-spheroids, describing well practically all forms of nanoparticles interesting for applications.

First of all, perfect nonradiating modes exist for a spherical particle of the radius R , having the following solution of the system (3),(4) for TM polarization:

$$\begin{aligned} H_\varphi &= j_n(z_0) j_n(k_0 \sqrt{\varepsilon} r) P_n^1(\cos \theta), r < R \\ H_\varphi &= j_n(z_1) j_n(k_0 r) P_n^1(\cos \theta), r > R \\ z_0 &= k_0 R; z_1 = k_0 \sqrt{\varepsilon} R \end{aligned} \quad (5)$$

where $P_n^1(\cos \theta)$ are Legendre polynomials.

Note that the condition for the existence of perfect nonradiating modes (5) has the form

$$\varepsilon j_n(z_1) [z_0 j_n(z_0)]' = j_n^{(1)}(z_0) [z_1 j_n(z_1)] \quad (6)$$

and coincides with the vanishing of the numerator of the Mie scattering coefficient.

Dispersion equation (6), along with complex roots, also has real roots, corresponding to perfect nonradiating modes. Fig. 1 shows the dependences of $\text{Re}(H_\varphi(r, \theta = \pi / 2))$ on the

radius for a perfect nonradiating mode and a usual mode with radiation losses in a sphere with $\varepsilon = 10$.

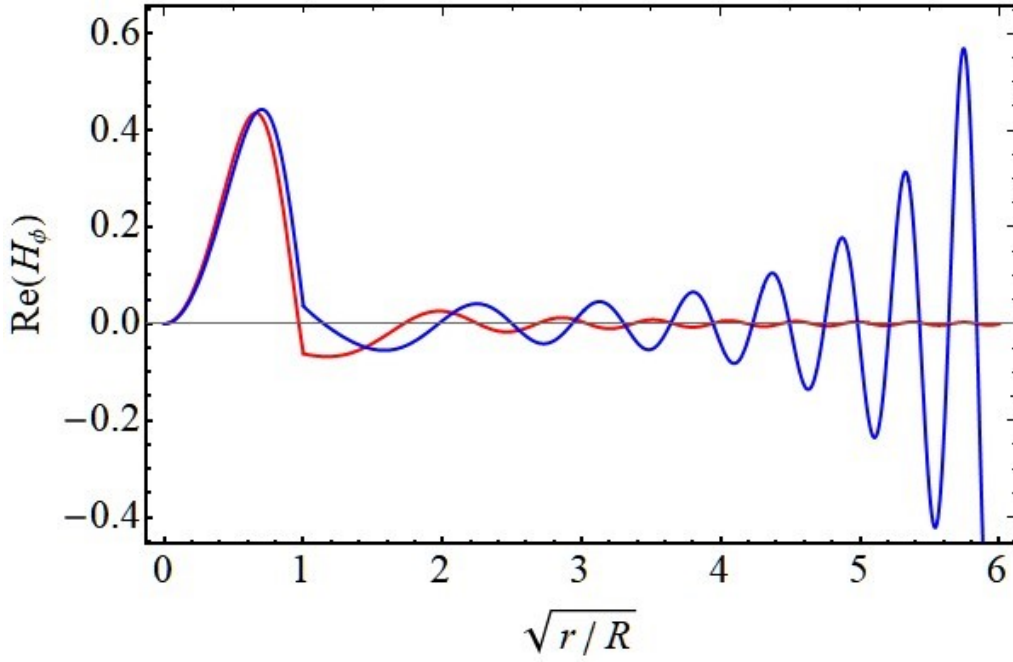


Fig. 1. The dependence of the magnetic field $\text{Re}(H_\phi(r, \theta = \pi/2))$ on the radius for the usual TM_{101} mode (blue curve, $k_0R=1.35715 - 0.160978i$) and for the perfect nonradiating PTM_{101} mode (red curve $k_0R=1.51893$) in a sphere with $\varepsilon = 10$.

Fig. 1 shows that the normal mode grows exponentially at infinity, while the perfect nonradiating mode goes to zero and has no radiation losses!

Nonradiating modes are not the feature of spherical geometry and, apparently, exist for axisymmetric open resonators of an arbitrary shape. We have shown rigorously that such modes exist for arbitrary spheroids with semiaxes a and b , having a volume equal to the volume of a sphere of the radius R with a surface described by the equation

$$(\rho/b)^2 + (z/a)^2 = 1; a = Rt^{2/3}; b = Rt^{-1/3} \quad (7),$$

where $t=a/b$. For $t < 1$, we have an oblate spheroid, and for $t > 1$, it is elongated.

The eigenfunctions and eigenfunctions of perfect nonradiating modes of such spheroids can be found by expanding the solutions of the equations (3) and (4) over spheroidal functions [39,40]. In the case of TM polarization for an elongated spheroid, the general solution of Maxwell's equations has the form

$$\begin{aligned}
H_{1,\varphi} &= \sum_{n=1}^{\infty} a_n PS_{n1}(c_1, \eta) S_{n1}(c_1, \xi), \\
H_{2,\varphi} &= \sum_{n=1}^{\infty} b_n PS_{n1}(c_0, \eta) S_{n1}(c_0, \xi)
\end{aligned} \tag{8}$$

where $PS_{n1}(c, \eta)$ are the angular spheroidal functions, $S_{n1}(c, \xi)$ are the radial spheroidal functions of the first kind, and $c_{0,1} = z_{0,1} \sqrt{t^2 - 1} / t^{1/3}$.

Equating the tangential components of the electric and magnetic fields on the surface of the spheroid (7) and using the orthogonality properties of angular spheroidal functions, one can find the dispersion equation describing the perfect nonradiating modes:

$$\begin{aligned}
\det M &= 0, \\
M_{np} &= \Pi_{np}(c_1, c_0) (\varepsilon SD_p(c_0, \xi_0) S_{n1}(c_1, \xi_0) - S_{p1}(c_0, \xi_0) SD_n(c_1, \xi_0))
\end{aligned} \tag{9}$$

where

$$\begin{aligned}
\Pi_{n,p}(c_1, c_0) &= \int_{-1}^1 d\eta PS_{n1}(c_1, \eta) PS_{p1}(c_0, \eta) \\
SD_n(c, \xi_0) &= \frac{\partial (\xi_0^2 - 1)^{1/2} S_{p1}(c, \xi_0)}{\partial \xi_0} \\
\xi_0 &= t / \sqrt{t^2 - 1};
\end{aligned}$$

Dispersion equation (9) is also valid for an oblate spheroid with the corresponding analytic continuation of spheroidal functions.

The exact solution of dispersion equations (9) for perfect TM modes (PTM) is shown in Fig. 2. This figure also shows the dispersion laws of usual TM modes and so-called confined modes [41] with magnetic field different from zero only inside the nanoparticle and conforming the equations:

$$\begin{aligned}
\nabla \times \nabla \times \mathbf{H}_n &= k_n^2 \mathbf{H}_n \quad \text{inside nanoparticle} \\
\mathbf{H}_n &= 0 \quad \text{at the boundary}
\end{aligned} \tag{10}$$

and the electric field of confined modes is zero everywhere.

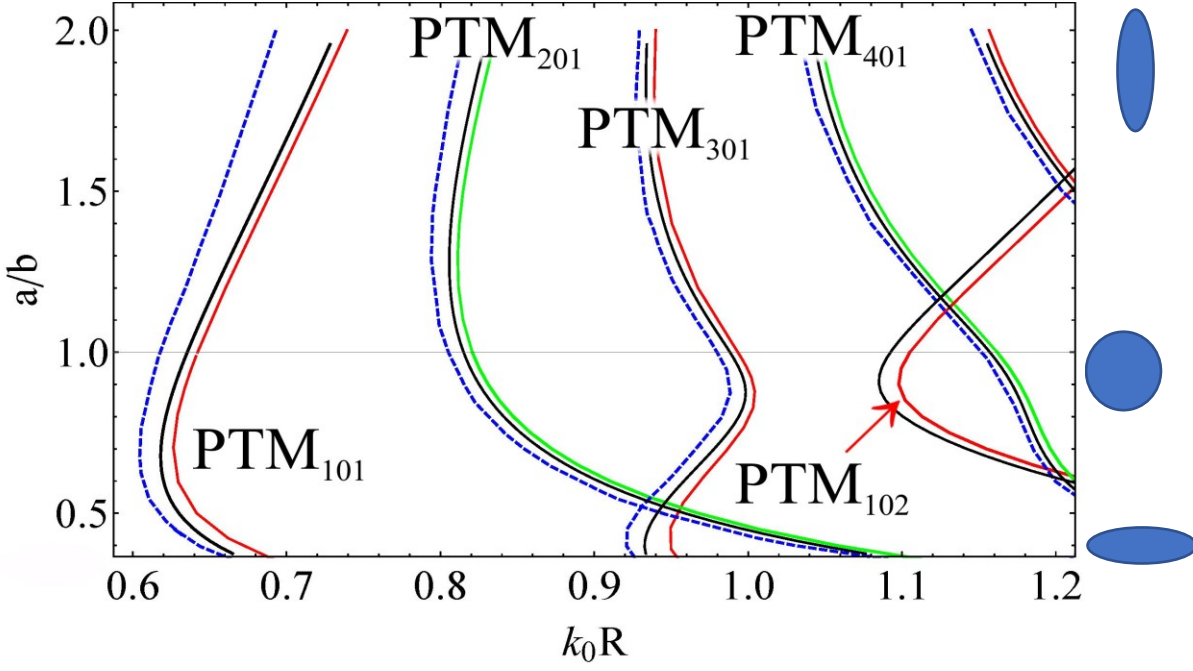


Fig.2. Perfect nonradiating TM modes (PTM) of spheroids with $\epsilon=50$ as a function of the size parameter k_0R and the spheroid aspect ratio, a/b . Red and green lines stand for odd and even perfect modes, blue dashed lines correspond to usual modes. Black lines show frequencies of confined modes (10), $\omega_{n,confined} = k_n c / \sqrt{\epsilon}$.

It can be seen from Fig. 2 that for each usual quasi-normal mode (blue dashed lines), there are its counterparts in the form of a perfect nonradiating mode (red and green lines) indicating that there are infinitely many perfect nonradiating modes. It should be emphasized here once again that the frequencies of the perfect nonradiating modes, the solution of (9), are real numbers!

Another interesting fact is that the eigenfrequencies of perfect nonradiating modes are slightly higher than the real parts of frequencies of usual modes $\omega_{n,usual}$. Moreover, it can be argued that the frequencies of confined modes (10), $\omega_{n,confined} = k_n c / \sqrt{\epsilon}$ (black curves), appearing in the limit of infinite permittivity, are always situated between the frequencies of usual and perfect nonradiating modes, $\omega_{n,usual} < \omega_{n,confined} < \omega_{n,perfect}$. This relationship between frequencies is a manifestation of a very deep connection between confined modes (with fields localized strictly inside the resonator) and perfect nonradiating modes (with fields not localized inside the resonator). Fig. 3 shows the dependence of the frequencies $k_0 R \sqrt{\epsilon}$ of usual and perfect nonradiating modes on the inverse permittivity.

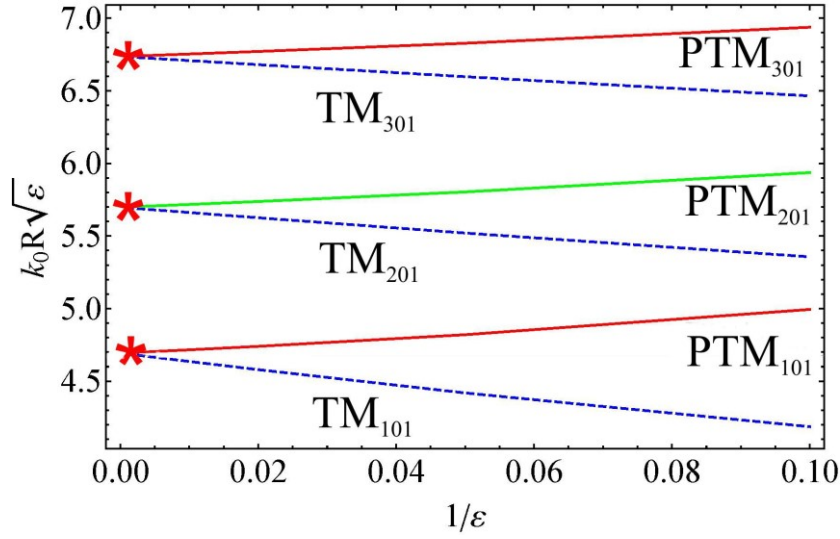


Fig. 3. Dependence of $k_0 R \sqrt{\epsilon}$ for usual and perfect nonradiating modes on $1/\epsilon$ for a spheroid with $a/b = 1.3$. The asterisks indicate confined modes (10).

From Fig. 3. it is seen that in the limit $\epsilon \rightarrow \infty$ the usual and perfect nonradiating modes merge into confined ones. However, at finite permittivities, this degeneracy is lifted, and confined modes are split into perfect nonradiating modes with infinite Q -factors and ordinary quasi-normal modes with finite Q -factors.

Such an unambiguous connection between the frequencies of confined modes and perfect nonradiating modes allows us to assert that perfect nonradiating modes with TM polarization exist for any axisymmetric dielectric bodies!

The found perfect nonradiating modes are not abstract solutions of sourceless Maxwell's equations. They are of great importance for finding the conditions for extremely small or even zero scattered power at a finite stored energy, leading to the unlimited radiative Q -factor. To demonstrate practical importance of perfect nonradiating modes, we have analyzed optical properties of nanospheroids of different shapes impinged by axially symmetric Bessel beam with TM polarization

$$H_\varphi \sim J_1(k_0 \sin \alpha \rho) \cos(k_0 z \cos \alpha) \quad (11)$$

where ρ and z are cylindrical coordinates and α is a conical angle of the beam.

In Fig. 4 one can see the dependence of scattered power P_{rad} , stored energy W_{stored} , and the generalized radiative quality factor $Q = \omega W_{stored} / P_{rad}$ on size parameter of nanospheroids for aspect ratio $a/b = 0.7$.

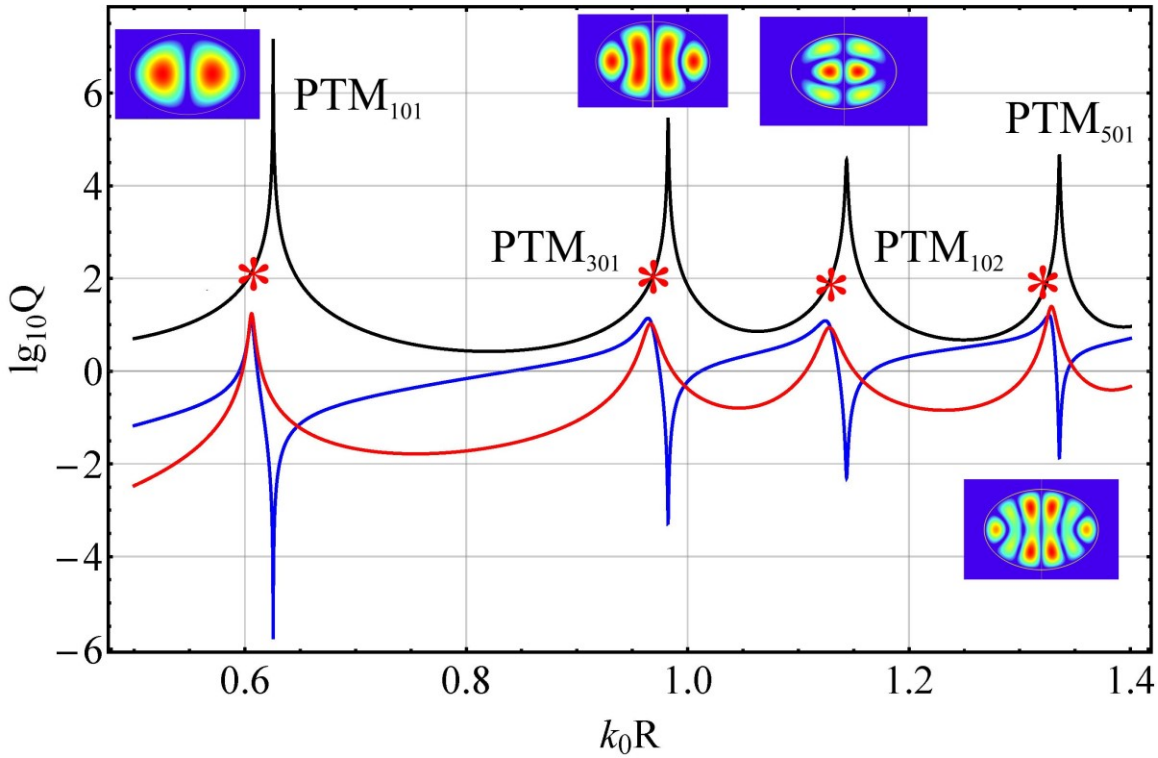


Fig.4. The dependence of scattered power P_{rad} (blue), stored energy W_{stored} (red), and generalized radiative Q factor (black) on the size parameter of an oblate spheroid with $a/b = 0.7$. TM symmetric excitation (11), $\alpha = \pi/4$, $\epsilon = 50$. The insets show the distribution of $|H_\varphi|$ corresponding to the Q -factor maxima. All maxima correspond to perfect nonradiating modes! The asterisks show the Q -factor of the usual modes.

Figure 4 shows clearly the presence of perfect nonradiating modes, having Q -factors significantly higher than usual ones. It can be seen from this figure that, upon excitation (11), all the maxima of the generalized Q -factor are due to perfect nonradiating modes. In this case, the Q -factors of usual modes (shown by asterisks) are several orders of magnitude lower than the Q -factors of perfect nonradiating modes! Moreover, smart optimization of the excitation beam [26] makes it possible to increase the Q factor of perfect nonradiating modes almost unlimitedly.

Above, as an example, perfect nonradiating PTM modes in dielectric spheroidal nanoparticles are considered. However, this approach is directly generalized to TE polarization and to other axisymmetric nanoparticles [42]. Moreover, this approach is directly generalized

to nanoparticles made from DNG or chiral metamaterials. However, the existence of perfect nonradiating modes for non-symmetric nanoparticles is still questionable.

In conclusion, we have put forward the concept of perfect nonradiating eigenmodes of light in dielectric nanoparticles. These modes are exact solution of sourceless Maxwell equations. We have shown rigorously that in the case of axisymmetric particles such modes always exist and arise at frequencies of somewhat higher resonance frequencies of usual modes.

Perfect nonradiating modes possess fully different physics than their weakly radiating counterparts and have no analogues. In particular, they differ from the so-called anapole modes [17-22,37] in that their field outside the particle is different from zero and has a well-defined expansion over spherical harmonics (2). These modes also differ from “bound states in a continuum” because they do not decay exponentially. The perfect modes are closest to strange Neumann-Wigner modes [38], but unlike the latter, the optical potential of a nanoparticle (permittivity) differs from vacuum value only in a finite region of space, fundamentally distinguishing perfect modes from Neumann-Wigner modes [38].

Due to unlimited radiative Q -factors our finding paves the way for development of new nano-optical devices with high concentration of field inside nanoparticles and extremely small radiative losses, including low threshold nanolasers, biosensors, parametric amplifiers, and nanophotonics quantum circuits.

Acknowledgments:

The reported study was funded by RFBR, project number 20-12-50136.

References

1. A. E. Krasnok, A. E. Miroshnichenko, P. A. Belov, and Y. S. Kivshar, *JETP Lett.* **94**, 593 (2011).
2. A. E. Krasnok, A. E. Miroshnichenko, P. A. Belov, and Y. S. Kivshar, *Opt. Express* **20**, 20599 (2012).
3. B. S. Luk'yanchuk, N. V. Voshchinnikov, R. Paniagua-Domínguez, and A. I. Kuznetsov, *ACS Photonics* **2**, 993 (2015).
4. E. Tiguntseva, K. Koshelev, A. Furasova, P. Tonkaev, V. Mikhailovskii, E. V. Ushakova, D. G. Baranov, T. Shegai, A. A. Zakhidov, Yu. Kivshar, and S. V. Makarov, *ACS Nano*, **14**, 7, 8149 (2020).

5. V. Mylnikov, S. T. Ha, Z. Pan, V. Valuckas, R. Paniagua-Dominguez, H. V. Demir, A. I. Kuznetsov, *ACS Nano* **14**, 7338 (2020).
6. W. Liu, A. E. Miroshnichenko, and Y. S. Kivshar, *Phys. Rev. B* **94**, 1(2016).
7. D. G. Baranov, D. A. Zuev, S. I. Lepeshov, O. V. Kotov, A. E. Krasnok, A. B. Evlyukhin, and B. N. Chichkov, *Optica* **4**, 814 (2017).
8. G. Grinblat, Y. Li and M.P. Nielsen et al., *ACSNano*, **11**, 953 (2017).
9. Yu. Kivshar, *National Science Review*, **5**, 144 (2018).
10. K. Koshelev, G. Favraud, A. Bogdanov, Yu. Kivshar, and A. Fratilocchi, *Nanophotonics*, **8**, 725 (2019).
11. Z. Sadrieva, K. Frizyuk, M. Petrov, Y. Kivshar, and, A. Bogdanov, *Phys. Rev. B* **100**, 115303, 1 (2019).
12. A. A. Bogdanov, *et al.*, *Adv. Photonics* **1**, 1 (2019).
13. K. Koshelev, *et al.*, *Science* **367**, 288 (2020).
14. L. Carletti, S. S. Kruk, A. A. Bogdanov, C. de Angelis, and Y. Kivshar, *Phys. Rev. Res.* **1**, 1 (2019).
15. L. Carletti, K. Koshelev, C. de Angelis, and Y. Kivshar, *Phys. Rev. Lett.* **121**, 33903 (2018).
16. Y. Yang, and S. I. Bozhevolnyi, *Nanotechnology*, **30**, 204001 (2019).
17. U. Manna, H. Sugimoto, D. Eggena, B. Coe, R. Wang, M. Biswas, and M. Fujii, *J. Appl. Phys.* **127**, 033101 (2020).
18. J. A. Parker, H. Sugimoto, B. Coe, D. Eggena, M. Fujii, N. F. Scherer, S. K. Gray, and U. Manna, *Phys. Rev. Lett.* **124**, 097402 (2020).
19. B. Luk'yanchuk, R. Paniagua-Domínguez, A. I. Kuznetsov, A. E. Miroshnichenko, and Y. S. Kivshar, *Phys. Rev. A.* **95**, 1 (2017).
20. L. Wei, Z. Xi, N. Bhattacharya, and H. P. Urbach, *Optica* **3**, 799 (2016).
21. A. E. Miroshnichenko, A. B. Evlyukhin, Y. F. Yu, R. M. Bakker, A. Chipouline, A. I. Kuznetsov, B. Luk'yanchuk, B. N. Chichkov, and Yu. S. Kivshar, *Nat. Commun.* **6**, 8069 (2015).
22. B. Luk'yanchuk, R. Paniagua-Domínguez, A. I. Kuznetsov, A. E. Miroshnichenko, and Y. S. Kivshar, *Philos. Trans. R. Soc. A Math. Phys. Eng. Sci.* **375**, 20160069 (2017).

23. Y. Lu, Y. Xu, X. Ouyang, M. Xian, Y. Cao, K. Chen, X.. Li, Cylindrical vector beams reveal radiationless anapole condition in a resonant state, arXiv:2104.10963 [physics.optics] (2021).
24. M. V. Rybin, K. L. Koshelev, Z. F. Sadrieva, K. B. Samusev, A. A. Bogdanov, M. F. Limonov, and Y. S. Kivshar, *Phys. Rev. Lett.* **119**, 243901 (2017).
25. M. Odit, K. Koshelev, S. Gladyshev, K. Ladutenko, Yu. Kivshar, and A. Bogdanov, *Adv. Mater.* **33**, 2003804 (2021).
26. V. Klimov, *Opt. Lett.* **45**, 4300 (2020).
27. F. Monticone, A. Alù, *Phys. Rev. Lett.* **112**, 213903 (2014).
28. C. Bohren and D. Huffman, *Absorption and Scattering of Light by Small Particles*, (John Wiley, New York, 1983).
29. P. T. Kristensen, C. van Vlack, and S. Hughes, *AIP Conf. Proc.* **1398**, 100–102 (2011).
30. P. T. Kristensen, and S. Hughes, *ACS Photonics.* **1**, 2–10 (2014).
31. C. Sauvan, J. P. Hugonin, I.S. Maksymov, and P. Lalanne, *Phys. Rev. Lett.* **110**, 237401(2013).
32. P. Lalanne, W. Yan, K.Vynck, C. Sauvan, and J. P. Hugonin, *Laser and Photonics Reviews* **12**, 1700113(2018).
33. E. A. Muljarov, and W. Langbein, *Phys. Rev. B* **94**, 235438 (2016).
34. R. Coccioli, M. Boroditsky, K. W. Kim, Y. Rahmat-Samii, and E. Yablonovitch, *IEE Proc. Optoelectron.* **145**, 391 (1998).
35. M. B., Doost, W. Langbein, and E.A. Muljarov, *Phys. Rev. A* **87**, 1 (2013).
36. C. Sauvan, *Opt. Express* **29**, 8268 (2021).
37. Ya. B. Zel'dovich, *JETP* **6**, 1184 (1957)
38. J. von Neumann and E. P. Wigner, *Physikalische Zeitschrift* **30**, 465(1929).
39. J. Meixner and F. W. Schäfke, *Mathieusche Funktionen und Sphäroidfunktionen mit Anwendungen auf physikalische und technische Probleme, Grundlehren der mathematischen Wissenschaften, Band 71*, Springer-Verlag, (1954)
40. Le-Wei Li, Xiao-Kang Kang, Mook-Seng Leong, *Spheroidal Wave Functions in Electromagnetic Theory*, John Wiley & Sons, Inc, (2002).
41. J. van Bladel, *MTT-23* 199 (1975).
42. See Supplemental Material at [] for details of calculations of perfect nonradiating modes in spheroids and hyperspheroids.

Supplementary material for the article
Perfect Nonradiating Modes in Dielectric Nanoparticles

Vasily Klimov

P.N. Lebedev Physical Institute, Russian Academy of Sciences, 53 Leninsky Prospekt,
Moscow 119991, Russia

E-mail: klimov256@gmail.com

1. Perfect nonradiating modes in dielectric spheroids

Apparently, perfect nonradiating modes exist for axisymmetric bodies of an arbitrary shape. It is shown strictly below that such modes exist for arbitrary spheroids with semiaxes a and b , having a volume equal to the volume of a sphere of the radius R and a surface described by the equation:

$$(\rho / b)^2 + (z / a)^2 = 1; a = Rt^{2/3}; b = Rt^{-1/3}, \quad (1),$$

where $t=a/b$. For $t < 1$, we have an oblate spheroid, and for $t > 1$, it is elongated.

The eigenfunctions and eigenfunctions of perfect nonradiating modes of such spheroids can be found by solving sourceless Maxwell's equations in elongated spheroidal coordinates ξ, η, φ [1,2], related to Cartesian coordinates by the equations:

$$\begin{aligned} x &= \frac{d}{2} (\xi^2 - 1)^{1/2} (1 - \eta^2)^{1/2} \cos \varphi \\ y &= \frac{d}{2} (\xi^2 - 1)^{1/2} (1 - \eta^2)^{1/2} \sin \varphi \\ z &= \frac{d}{2} \xi \eta; d = 2\sqrt{a^2 - b^2} \end{aligned} \quad (2)$$

In these coordinates, the surface of the spheroid (1) is determined by the condition:

$$\xi = \xi_0 = a / \sqrt{a^2 - b^2}.$$

In elongated spheroidal coordinates, the Lamé coefficients have the form [2]:

$$h_\xi = \frac{d}{2} \sqrt{\frac{\xi^2 - \eta^2}{\xi^2 - 1}}; h_\eta = \frac{d}{2} \sqrt{\frac{\xi^2 - \eta^2}{1 - \eta^2}}; h_\varphi = \frac{d}{2} \sqrt{(\xi^2 - 1)(1 - \eta^2)} \quad (3)$$

In spheroidal coordinates, the variables can be separated, and solutions of Maxwell's equations can be represented as an expansion over spheroidal wave functions.

1.1 TM polarization, non-magnetic case

In the case of TM polarization, for a single nonzero component of the magnetic field, we can write

$$H_{1,\varphi} = \sum_{n=1}^{\infty} a_n PS_{n1}(c_1, \eta) S_{n1}(c_1, \xi), c_1 = k_0 R \sqrt{\varepsilon} \sqrt{t^2 - 1} / t^{1/3} \text{ inside nanoparticle, } \xi < \xi_0$$

$$H_{2,\varphi} = \sum_{n=1}^{\infty} b_n PS_{n1}(c_0, \eta) S_{n1}(c_0, \xi), c_0 = k_0 R \sqrt{t^2 - 1} / t^{1/3} \text{ outside nanoparticle, } \xi > \xi_0$$

where $PS_{n1}(c, \eta)$ are the angular spheroidal functions, $S_{n1}(c, \xi)$ are the radial spheroidal functions of the first kind [1].

The tangential component of the electric field

$$E_\eta = \frac{i}{k_0 \varepsilon} \frac{1}{h_\xi h_\varphi} \frac{\partial h_\varphi H_\varphi}{\partial \xi} \quad (4)$$

looks like:

$$E_{1,\eta} = \frac{1}{\varepsilon} \frac{2i}{k_0 d (\xi^2 - \eta^2)^{1/2}} \sum_{n=1}^{\infty} a_n PS_{n1}(c_1, \eta) \frac{\partial (\xi^2 - 1)^{1/2} S_{n1}(c_1, \xi)}{\partial \xi} \quad (5)$$

inside nanoparticles, $\xi < \xi_0$, and

$$E_{2,\eta} = \frac{2i}{k_0 d (\xi^2 - \eta^2)^{1/2}} \sum_{n=1}^{\infty} b_n PS_{n1}(c_0, \eta) \frac{\partial (\xi^2 - 1)^{1/2} S_{n1}(c_0, \xi)}{\partial \xi} \quad (6)$$

in its exterior, $\xi > \xi_0$.

After multiplication by angular harmonics, integration over η , and application of the orthogonality condition for angular spheroidal functions,

$$\int_{-1}^1 d\eta PS_{n1}(c_1, \eta) PS_{m1}(c_1, \eta) = \delta_{nm} NN_n = \delta_{nm} \frac{2n(n+1)}{2n+1} \quad (7)$$

the conditions for the continuity of the magnetic field at the spheroid boundary take the form:

$$a_n NN_n S_{n1}(c_1, \xi_0) = \sum_{p=1}^{\infty} \Pi_{np}(c_1, c_0) S_{p1}(c_0, \xi_0) b_p \quad (8)$$

Similarly, the boundary conditions for the continuity of the electric field at the boundary of the spheroid $\xi = \xi_0$ can be written in the form:

$$\frac{1}{\varepsilon} a_n NN_n SD_n(c_1, \xi_0) = \sum_{p=1}^{\infty} \Pi_{np}(c_1, c_0) SD_p(c_0, \xi_0) b_p, \quad (9),$$

were

$$SD_n(c, \xi_0) = \frac{\partial(\xi_0^2 - 1)^{1/2} S_{p1}(c, \xi_0)}{\partial \xi_0} \quad (10).$$

In (8) and (9)

$$\Pi_{n,p}(c_1, c_0) = \int_{-1}^1 d\eta PS_{n1}(c_1, \eta) PS_{p1}(c_0, \eta) \quad (11)$$

stands for the overlap integral of angular spheroidal functions for different c_1 and c_0 .

Figure S1 shows the dependence of the overlap integral of angular spheroidal functions $\Pi_{n,p}(c_1, c_0)$ on the indices n, p .

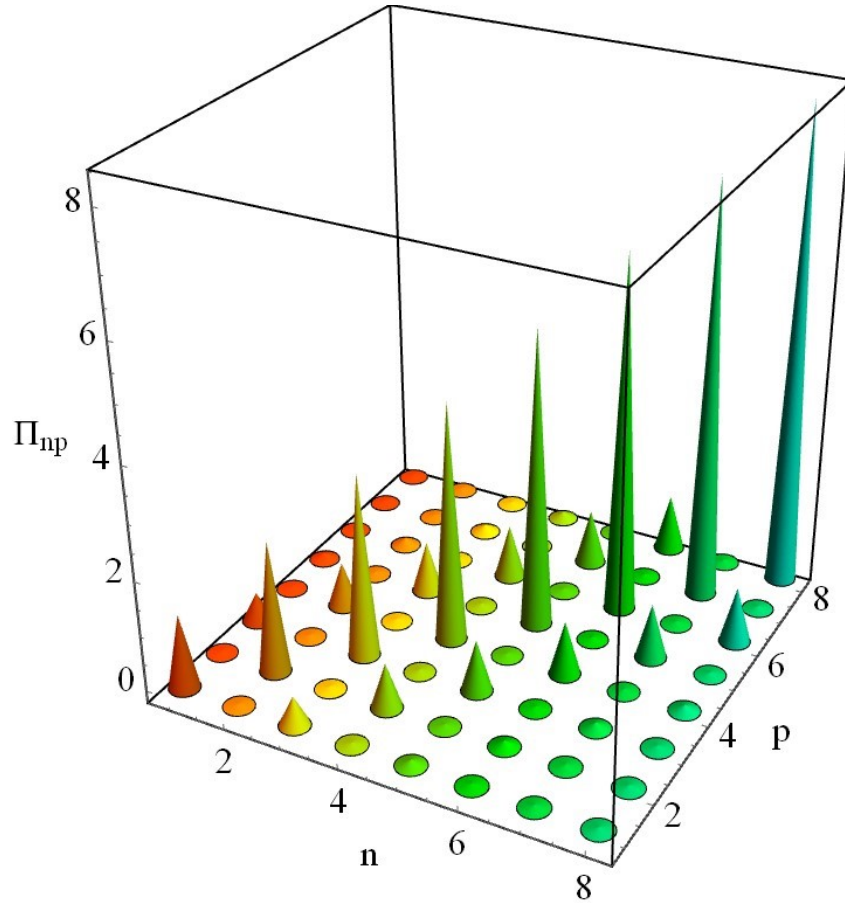


Fig. S1. Dependence of the overlap integral of angular spheroidal functions in an elongated spheroid $\Pi_{n,p}(c_1, c_0)$ on indices. $c_1 = 4, c_0 = c_1 / \sqrt{\varepsilon} = 0.5657, \varepsilon = 50$

Figure S1 shows that:

- 1) only modes with the same parity interact with each other;
- 2) for each mode, interaction is essential only with the nearest modes of the same parity, $2k \Leftrightarrow 2(k \pm 1); 2k + 1 \Leftrightarrow 2(k \pm 1) + 1$. This circumstance simplifies calculations since matrices of finite dimension 3×3 can be used to calculate eigenfrequencies.

Eliminating a_n from (8) and (9), we obtain a homogeneous system for the coefficients b_p , determining the magnetic field outside the particle:

$$\sum_{p=1}^{\infty} \Pi_{np}(c_1, c_0) (\varepsilon S D_{p1}(c_0, \xi_0) S_{n1}(c_1, \xi_0) - S_{p1}(c_0, \xi_0) S D_{n1}(c_1, \xi_0)) b_p = 0 \quad (12),$$

The compatibility condition of (12) allows one to find the modes and eigenfrequencies of the perfect nonradiating modes shown in Fig. 2 of the article.

1.2. TE polarization, non-magnetic case

In this case, the only nonzero component of the electric field can be written in the form:

$$E_{1,\varphi} = \sum_{n=1}^{\infty} a_n P S_{n1}(c_1, \eta) S_{n1}(c_1, \xi), c_1 = k_0 R \sqrt{\varepsilon} \sqrt{t^2 - 1} / t^{1/3} \text{ inside nanoparticle, } \xi < \xi_0 \quad (13)$$

$$E_{2,\varphi} = \sum_{n=1}^{\infty} b_n P S_{n1}(c_0, \eta) S_{n1}(c_0, \xi), c_0 = k_0 R \sqrt{t^2 - 1} / t^{1/3} \text{ outside nanoparticle, } \xi > \xi_0$$

Repeating the reasoning for TM polarization, for the coefficients b_p , determining the electric field outside the particle, we obtain a homogeneous system of equations:

$$\sum_{p=1}^{\infty} \Pi_{np}(c_1, c_0) (S_{D_{p1}}(c_0, \xi_0) S_{n1}(c_1, \xi) - S_{p1}(c_0, \xi_0) S_{D_{n1}}(c_1, \xi_0)) b_p = 0 \quad (14)$$

that differs from the dispersion equation (12) only by the absence of ε in the parenthesis.

The compatibility condition of (14) allows one to find the eigenfrequencies of perfect nonradiating modes with TE polarization (see Fig. S2).

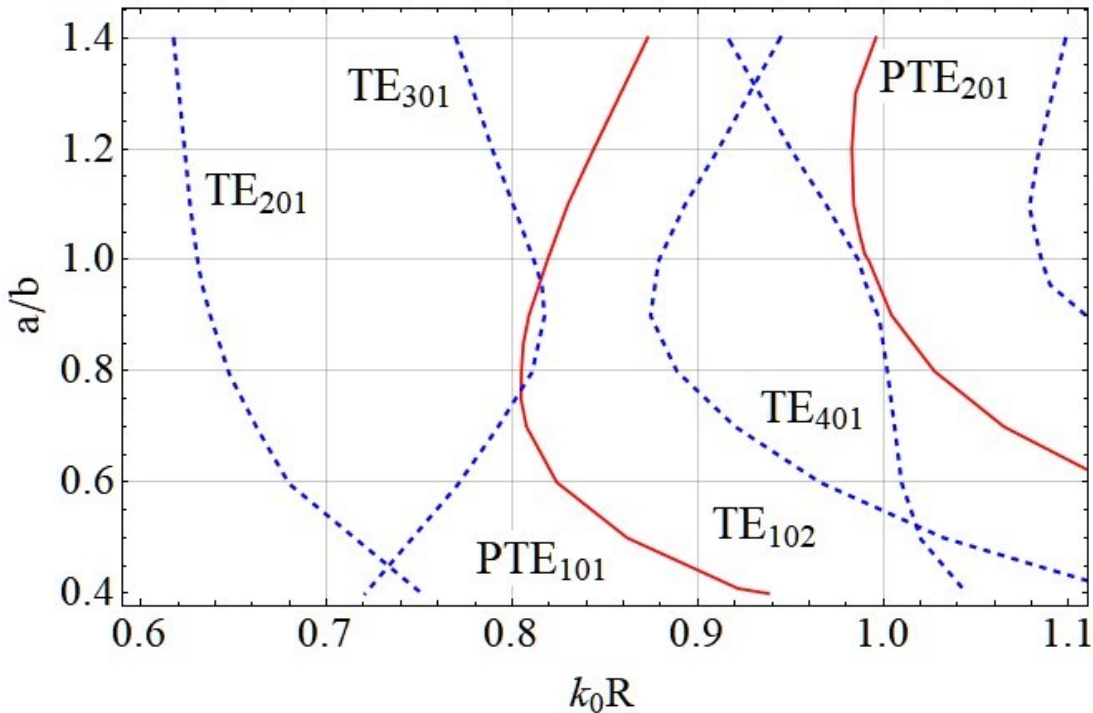


Fig.S2. Perfect nonradiating TE modes of spheroids with $\varepsilon=50$ as a function of the size parameter k_0R and the aspect ratio of ellipsoid, a/b . Red curves stand for TE perfect nonradiating modes (PTE), blue dashed lines correspond to usual TE modes.

From Fig. S2 and the structure of dispersion equation (14), it follows that the number of perfect non-emitting modes with TE polarization is infinite, as in the case of TM polarization.

Demonstration of the existence of TE perfect nonradiating modes is more complicated in comparison with the TM case, since perfect modes with TE polarization are not confined modes [3] in the limit $\varepsilon \rightarrow \infty$. In addition, the frequencies of perfect PTE_{n,0,1} modes turn out to be close to the frequencies of usual TE_{n+1,0,1} modes. Therefore, to demonstrate perfect nonradiating TE modes, an incident beam should not excite usual nearby modes. In particular, to demonstrate the existence of the PTE₁₀₁ mode (see Fig.S3), it is necessary to suppress the excitation of the usual TE₃₀₁ mode, by using an exciting field of the form:

$$E_\varphi(R, \theta) \sim (j_1(k_0 R) P_1^1(\theta) + \xi j_3(k_0 R) P_3^1(\theta)) \quad (15)$$

In (15), R and θ are spherical coordinates, $j_n(z)$ and $P_n^l(\cos \theta)$ are the spherical Bessel functions and the Legendre polynomial, correspondingly.

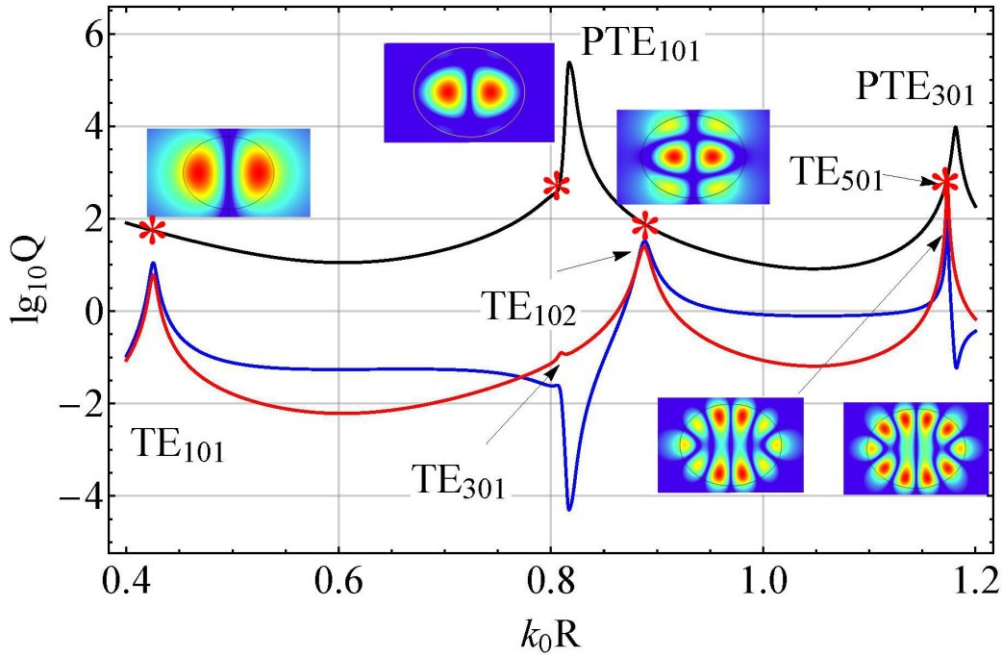


Fig.S3. The dependence of scattered power (blue), stored energy (red), and Q -factor (black) on the size parameter of nanoparticles. TE excitation (15), $\xi=-9.915$, $\varepsilon=50$. $a/b=0.8$ (oblate spheroid). The asterisks show the Q values of usual modes.

Fig. S3 clearly shows the presence of perfect nonradiating modes, having Q -factors significantly higher than the Q -factors of usual modes. Moreover, smart optimization of the

excitation beam [4] makes it possible to increase the Q -factor of perfect nonradiating modes unlimitedly (with neglect of Joule losses in the nanoparticle material, of course).

2. Perfect nonradiating modes in a cylinder: TM polarization

We have not yet succeeded in finding an analytical solution for perfect nonradiating modes in a dielectric cylinder of a finite height. However, proceeding from the very plausible hypothesis that the existence of perfect modes is associated with the existence of confined modes, we have found the frequencies of perfect nonradiating modes by simulating the scattering of a Bessel beam

$$H_\varphi \sim J_1(k_0 \sin \alpha \rho) \cos(k_0 z \cos \alpha) \quad (16)$$

by a hyperspheroid with the surface described by the equation:

$$\left(\rho / a(t)\right)^t + \left(z / c(t)\right)^t = 1 \quad (17)$$

For $t = 2$, this is a sphere: $a(2) = c(2) = R$:

$$\rho^2 / R^2 + z^2 / R^2 = 1 \quad (18)$$

At $t = \infty$, this is a cylinder with the diameter $2a(\infty) = D_{cyl}$ and the height $H_{cyl} = 2c(\infty)$

In Fig. S4, one can see the dependence of scattered power, stored energy, and Q -factor on the size parameter k_0R of a hyperspheroid with $t = 8$ when excited by a Bessel beam (16).

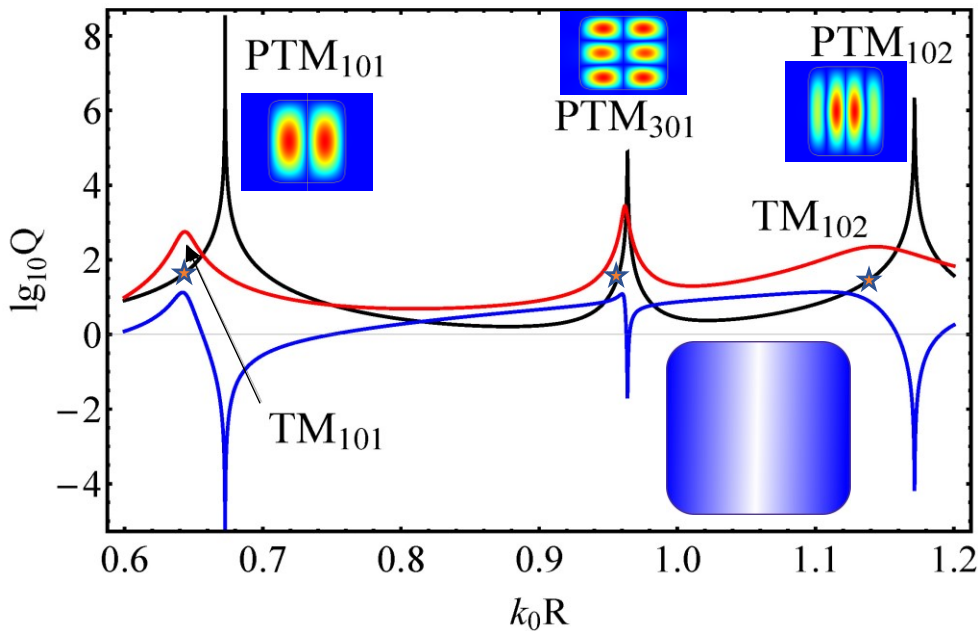


Fig.S4. The dependence of scattered power (blue), stored energy (red), and Q -factor (black) on the size parameter of a hyperspheroid with $D/H=0.96$, $t=8$. TM symmetric excitation (16), $\varepsilon=50$, $\alpha=\pi/4$. The insets show the field distribution corresponding to the Q -factor maxima and the shape of the investigated hyperspheroid. All maxima correspond to perfect nonradiating modes! The asterisks show the Q -factor values of usual modes.

Fig. S4 shows that all the maxima of the generalized Q -factor with the excitation (16) are due to perfect nonradiating modes, with Q -factors of several orders of magnitude higher than the Q -factors of usual modes.

References

1. J. Meixner and F. W. Schäfke, Mathieusche Funktionen und Sphäroidfunktionen mit Anwendungen auf physikalische und technische Probleme, Grundlehren der mathematischen Wissenschaften, Band 71, Springer-Verlag, (1954)
2. Le-Wei Li, Xiao-Kang Kang, Mook-Seng Leong, Spheroidal Wave Functions in Electromagnetic Theory, John Wiley & Sons, Inc, (2002).
3. J. van Bladel, On the resonances of a dielectric resonator of very high permittivity, IEEE transactions on microwave theory and techniques, MTT-23 199 (1975).
4. V. Klimov, Manifestation of extremely high- Q pseudo-modes in scattering of a Bessel light beam by a sphere, Opt. Lett. 45, 4300 (2020).